Indian Journal of Engineering & Materials Sciences
Vol. 19, August 2012, pp. 237-244

Hybrid composite materials of anatase titania and conducting polyaniline: properties and chemical sensor application

E Subramanian[a]*, R Dhana Ramalakshmi[a], N Vijayakumar[b] & G Sivakumar[c]

[a]Department of Chemistry, Manonmaniam Sundaranar University, Tirunelveli 627 012, India

[b]Department of Physics, Sri K.G.S. Arts College, Srivaikuntam, Thoothukudi 628 619, India

[c]CISL, Department of Physics, Annamalai University, Annamalai Nagar, 608 002, India

Received 20 December 2011; accepted 26 June 2012

This paper reports the investigation on synthesis, properties and chemical sensor application of polyaniline (PANI) - anatase titania (TiO_2) hybrid composite materials prepared in the presence and absence of the soft template poly (vinyl alcohol) (PVA). FTIR spectroscopy reveals that PVA favors oxidation of large amount of aniline during PANI synthesis and causes production of more number of quinoid groups than benzenoid, but TiO_2 maintains an equal level of quinoid and benzenoid. XRD study shows that PVA influences the *d*-space and crystallite size more in PANI-PVA and less in PANI-TiO_2-PVA composite. In morphology, PANI-TiO_2 has submicron particles and shows less agglomeration while PANI-TiO_2-PVA has extensive agglomeration and surface smoothness. In chemical sensor application, PANI senses CH_3OH vapor with a decrease of its conductivity and with an efficiency of 56%. However, with the inclusion of TiO_2 or PVA, the sensor efficiency of PANI is shifted from CH_3OH to CH_2Cl_2. Interestingly with both TiO_2 and PVA inclusion, the material PANI-TiO_2-PVA turns back its maximum sensor efficiency towards CH_3OH but with an increase of its conductivity. All these results suggest that TiO_2, PVA and TiO_2-PVA exert different tuning roles on PANI yielding characteristically different hybrid materials.

Keywords: Polyaniline, Titania, Hybrid composites, Chemical sensor

Organic-inorganic hybrid composite (OIHC) materials have been receiving a great deal of attention in recent years[1-8] because such materials with new properties and features facilitate the development of innovative industrial applications[4]. The properties of OIHC materials are not simply the addition of properties of the two components, but many new features arise through synergistic behavior[7,8]. For example, in nature many biomaterials gain their exceptional strength and toughness from the combination of inorganic material with an organic matrix[9].

Intrinsically conducting polymers (ICPs) are conjugated organic molecular systems and the π-electron backbone present in them is responsible for their novel electronic and electrical properties[10]. Their list of applications covers a wide spectrum[11,12] and hence in recent years they receive a considerable attention of scientific and technological interest[11,13]. For example, ICPs are widely used in chemical and biological sensors, with greater sensitivity and versatility[10]. Among the conducting polymers, polyaniline (PANI) is a unique and prominent material[13]. OIHC materials involving PANI can be easily prepared by incorporating metallic components, e.g., metal oxides in to PANI. Through the formation of such OIHC materials, and the existence of synergistic behavior of the two components[7,8], the properties of conducting PANI can be varied. PANI OIHC materials are, therefore, found to be suitable for many applications. Particularly PANI-TiO_2 (titania) composites are applied in corrosion protection coatings[14], solar cells[15,16], photocatalysis[17,18] and microwave absorption[19].

Generally, studies on PANI-TiO_2 composites are limited. Also the utilization of crystalline titania (TiO_2 with anatase structure) in composite preparation is found to be very rare. Hence, in the present work OIHC materials of PANI-TiO_2 were prepared and studied. Poly(vinyl alcohol) (PVA) is a water-soluble polymer. Using its –OH group it can form hydrogen bonding with H_2O or amine/imine groups of polyaniline chain. When it forms such intermolecular H-bond crosslinks with oligomeric or growing polyaniline chain, it can control the stereochemistry of the polymer molecule and ultimately the polyaniline particle size and morphology. Because of

*Correspondence author (E-mail: esubram@yahoo.com)

this functionality in the dissolved state, PVA is termed as a soft template[20-22]. Hence, the influence of PVA soft template on the properties of OIHC materials is also of interest.

A total four materials PANI, PANI-TiO_2, PANI-PVA and PANI-TiO_2-PVA were synthesized and studied for their chemical sensor properties towards solvent vapors of volatile organic compounds (VOC). The inorganic and organic components (TiO_2 and PVA) tune the physico-chemical properties of PANI and accordingly the chemical sensor properties of hybrid composites are modified. Interesting results are obtained concerning the roles of TiO_2 and/or PVA whereby the study provides an understanding of the relationship between the tuning effects and properties of the hybrid materials.

Materials and Methods

Materials

Aniline, GR grade from Merck was distilled over Zn dust and used. TiO_2 99.8% anatase powder from Aldrich was used as such. PVA (MW ~ 14,000) was from S.D. Fine-Chem. Concentrated (con.) H_2SO_4, ammonium peroxydisulfate (APS), organic solvents and other reagents were of analytical grade and were used without any purification. Double-distilled water was used throughout the experiment.

Methods

Synthesis of PANI and its composites

PANI and its composite materials were synthesized by chemical oxidative polymerization technique, with APS oxidant. The conventional method[23] followed earlier[24-26] was slightly modified, particularly in the reduction of total volume (200 mL) of the polymerization mixture. Since anatase powder cannot distribute uniformly throughout the whole volume (as it tends to settle down), the volume was maintained as low as possible (~ 15 mL) in order to ensure the uniform disperse of TiO_2 powder on stirring. The typical procedure is as follows. 2 mL of distilled aniline was mixed with 2 mL of con. H_2SO_4 and the mixture was diluted with 10 mL of double-distilled water. 0.5 g of anatase TiO_2 powder without/with 0.12 g of PVA template (molar stoichiometric ratio of PVA : Aniline = 0.1 : 1) was added to the aniline sulfate solution and dispersed through constant stirring with a magnetic stirrer. The whole mixture was maintained at 0-5°C in ice-bath and stirred for 30 min. 4 g of APS solid (oxidant: aniline ratio = 1:1) was slowly added to the cold aniline sulfate solution and stirring was continued further for 3- 4 h at 0-5°C. The mixture was placed inside a refrigerator overnight for completion of polymerization and precipitation. The next day it was washed with copious amount of double distilled water and 0.1 M H_2SO_4 till the filtrate became colorless. The polymer sample was dried in a vacuum oven at 110-120°C for 4-5 h, ground into a fine powder and stored in air-tight polythene covers.

The control polymer materials, pristine PANI and PANI-PVA were also synthesized in a similar way without TiO_2 but in the absence and presence of 0.12 g of PVA, respectively.

Characterization of PANI composites

FTIR spectra of the powdered polymer samples were recorded in spectral grade KBr pellet with JASCO FTIR-410 spectrometer in the wavenumber range 400-4000 cm^{-1} at a resolution of 2 cm^{-1}. Powder X-ray diffraction patterns were obtained for the angle 2θ = 10-80° in a step of 0.05° with the instrument PANalytical Expert Pro-MPD with CuK_α radiation (λ = 1.5406 Å) from a generator set at 30 mA and 40 kV. For scanning electron micrograph, samples were first coated with a thin layer of gold for 120 s from a Jeol auto fine coater model JFS-1600 and pictures were obtained using the instrument Jeol JSM 5610 LV (15/20 KV) at a magnification of 10000×. DC electrical conductivities of the polymer samples were measured by the standard collinear four-point probe method[27]. Pellets of dimension 13 × 2 mm were made with manual hydraulic press at 4 metric ton pressure and *I-V* values were measured by making gentle contact of the pellet with collinear four-point probe at different positions and drawing current from a constant power supply unit (Scientific Equipment & Services, Model DFP – 02). 1/*R* values were computed from the *I-V* values, and using average 1/*R* values, conductivities were calculated using Eq. (1).

$$\text{Conductivity } (\sigma) = 1/2\ \pi RS \qquad \ldots (1)$$

where *R* is the resistance and *S* is the distance between the two probes (2 mm).

Sensor studies in static and dynamic methods

The sensor experiment in static method was performed by exposing the pellet to saturated vapors of various organic solvents, CH_3OH, CH_2Cl_2, CH_3CN and DMSO (VOCs) for about 30 min inside an air-removed and solvent-vapor-filled vacuum

desiccators and measuring the *I-V* values of the pellet before and after exposure at room temperature. The exposure time was more than the pre-determined equilibration time (~20 min). On re–exposure to air, the vapor left the pellet by evaporation and the volt returned to its original value. The sensor efficiency was determined by the normalized voltage change as denoted by Eq. (2).

$$\text{Sensor efficiency, } \eta = [(V_s - V_a)/V_a] \times 100 \quad \ldots (2)$$

where V_s and V_a are the voltage of the pellet with solvent and air exposure, respectively.

In dynamic sensor study, pellet with four collinear contacts made of enameled copper wires and conducting silver paste (two for current and two for volt measurement) was exposed to a flow of solvent vapor with air as carrier inside a closed chamber for a particular period of time. Voltage was measured during exposure to the flow of pure air or solvent vapor mixture against time in a digital multimeter. Air-exposure and solvent-exposure were thus made alternatively and the sensor response in volt was recorded for 3-4 cycles.

Results and Discussion

IR spectral characterization

Figure 1 shows the FTIR spectra of all the four PANI materials. The characteristic vibrations of PANI, namely the stretching of quinoid, benzenoid and imine groups and the in-plane and out-plane bending of C–H bonds of quinoid and benzenoid[16] occur at 1602, 1482, 1301, 1114 and 789 cm^{-1}, respectively (Fig. 1a). The quinoid and benzenoid stretchings appear relatively at higher wave numbers while the C-H out-plane bending at lower side by almost 10-20 cm^{-1} when compared to the normally-observed positions[13,28-30]. Also the intensity of quinoid is about twice that of benzenoid, showing qualitatively a greater level of aniline oxidation and the consequent more number of quinoid groups than benzenoid in pristine PANI. However, in TiO_2 composite the PANI spectrum (Fig. 1b) almost returns to its normal position with more or less equal quinoid and benzenoid intensities. With PVA soft template alone or together with TiO_2 matrix, i.e., in PANI-PVA and PANI-TiO_2-PVA composites, the PANI spectra (Fig. 1c, d) continue to follow the trend of pristine PANI (Fig. 1a) to a greater extent. Therefore, the quinoid/benzenoid intensity ratio in PANI-PVA and PANI-TiO_2-PVA composites also becomes higher than that of pristine PANI. That means the addition of soft template PVA favors an oxidation of large amount of aniline during PANI synthesis and causes production of more number of quinoid groups than benzenoid.

XRD characterization

XRD patterns of all PANI materials are shown in Fig. 2 and the data computed from these patterns are given in Table 1. Of the four PANI materials, PANI and PANI-PVA show broad peaks while PANI-TiO_2 and PVA templated PANI-TiO_2-PVA materials show very sharp signals. The XRD patterns of PANI and PANI-PVA, appear similar in shape (Fig. 2 a and c). However, PANI pattern (Fig. 2a) is found to be

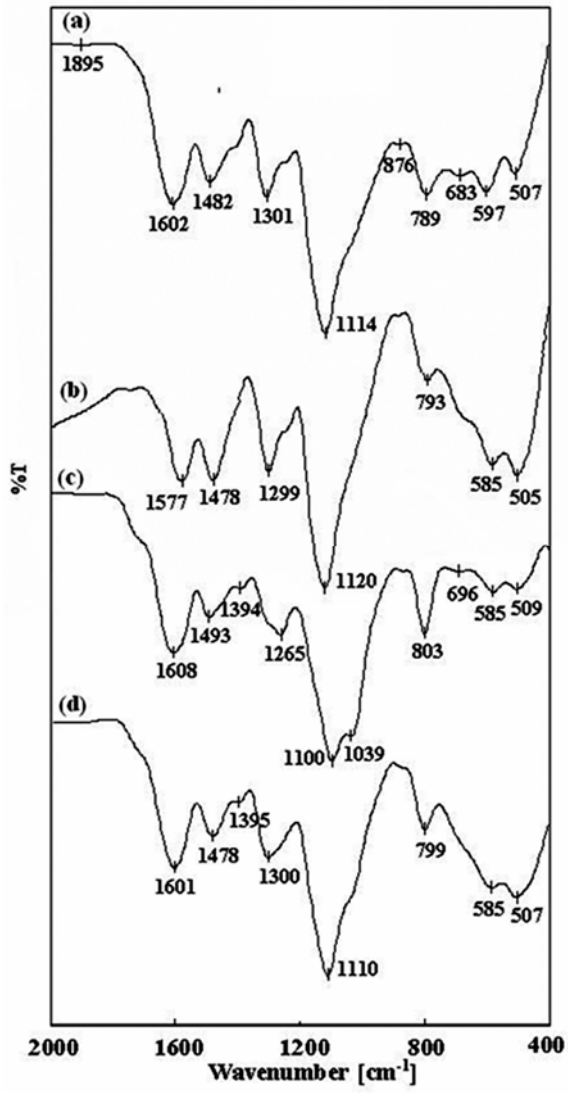

Fig. 1—FTIR spectra of (a) PANI, (b) PANI-TiO_2, (c) PANI-PVA and (d) PANI-TiO_2-PVA materials

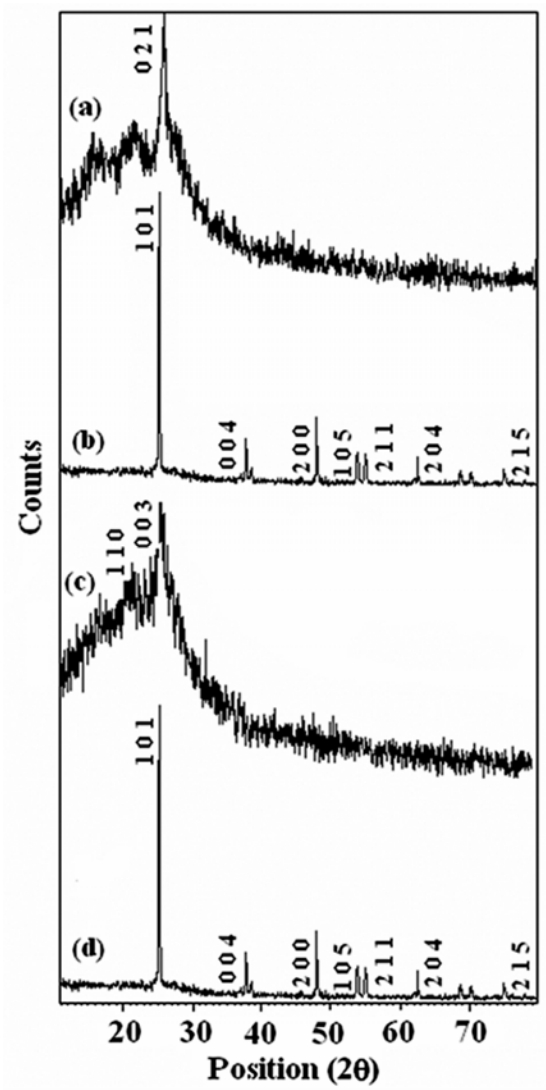

Fig. 2—XRD patterns of (a) PANI, (b) PANI-TiO_2, (c) PANI-PVA and (d) PANI-TiO_2-PVA materials

Table 1—XRD data of PANI materials

Sample	Position (2θ)	*d* – space (Å)	FWHM × 10^{-3} (rad)	D (nm)
PANI	25.113	3.543	29.3	4.85
PANI–TiO_2	25.209	3.530	2.18	65.21
PANI–PVA	25.152	3.538	24.2	5.88
PANI–TiO_2+PVA	25.222	3.528	2.28	62.27

matchable with the polyaniline XRD pattern reported in JCPDS File no. 53–1891 while PANI-PVA pattern (Fig. 2c) has matching with the polyaniline XRD pattern in JCPDS File no. 53–1717. The two JCPDS files report the XRD patterns of two previously studied polyaniline materials, respectively both having the same orthorhombic crystalline structure. But polyaniline in File no. 53-1891 has only one XRD peak while polyaniline in File no. 53-1717 has been reported with two XRD peaks. From the matching it is concluded that both PANI and PANI-PVA have the same orthorhombic crystalline structure. But differences are noticeable in the number of XRD reflections, *d*-space, FWHM and the crystallite size values (Table 1). The former has only one (*h k l*) assignable signal (0 2 1) but the latter has two signals (0 0 3 and 1 1 0). The highest intensity peak at about 25º occurs at lower *d*-space and lower FWHM in PANI-PVA relative to PANI so that PANI-PVA has somewhat bigger average crystallite size than PANI. Thus, PVA inclusion in PANI greatly influences its structure and makes PANI-PVA a material of close-packed crystalline planes and bigger crystallite size.

For PANI-TiO_2 and PANI-TiO_2-PVA composites, the XRD pattern of anatase TiO_2 reported in JCPDS File No. 71–1767 is found to be matchable. There is good agreement between the pattern reported in JCPDS file and the two observed XRD patterns (Fig. 2b, d) in terms of sharp high intense reflections, peak positions and (*h k l*) values of the respective planes. This implies that the anatase crystalline structure of free TiO_2 is possessed by the above two TiO_2 composites and also that the anatase TiO_2 structure is not much influenced. Previous study[17] has also witnessed such observation. Nevertheless, fine differences do exist between PANI-TiO_2 and PANI-TiO_2-PVA in *d*-space and average crystallite size values which are marginally lower for latter. Therefore, it is inferable that PVA exhibits only very minor influence on structure and particle sizes of PANI-TiO_2 composite.

SEM characterization

The scanning electron micrographs are shown in Fig. 3. Pristine PANI is seen with rough surfaced, fractured and extensively agglomerated large solid clumps (Fig. 3a). For PANI-TiO_2 hybrid material the image clearly shows the presence of spherically shaped primary particles of submicron/nanometer size and their agglomeration into secondary particles/grains of various sizes. It is also seen that a TiO_2 micron size particle is fully covered by nanometer-sized PANI primary particles as white dots/patches. Another notable feature in PANI-TiO_2 hybrid material image is that agglomeration is less extensive compared to PANI so that grains of clear shape and size are visible (Fig. 3b). PANI-PVA composite shows clearly a distinct image consisting of bigger grains with white patches and smooth surface (Fig. 3c). Enhanced

agglomeration and surface smoothness caused by PVA are seen in the image of PANI-TiO_2–PVA (Fig. 3d) where the primary particles appearance is less visible compared to that in PANI-TiO_2. The enhanced agglomeration of PVA template is in conjunction with its role observed in XRD characterization. The lower *d*-space caused by PVA in both PANI-PVA and PANI-TiO_2-PVA materials could make the polymer chains close and support agglomeration.

Conductivity properties

DC electrical conductivity values of all the PANI materials at room temperature are given in Table 2. PANI has a moderately low value of 0.26 Scm^{-1} which may be attributed to the extensive agglomeration and the resultant disordered arrangement of polymer chains. Incorporation of TiO_2 and/or PVA in PANI composites further reduces the conductivity value and this is understandable by the fact that the added materials are poor/non-conductors. Karim *et al.*[31] have observed a conductivity value of 0.28 Scm^{-1} for bulk PANI and 0.15 Scm^{-1} for PANI-TiO_2 composite submicron rods synthesized by using an *in situ* γ-irradiation induced chemical polymerization method. These conductivity values are close to the values of present work. In another study[32] a similar trend in conductivities has been reported.

Table 2—Conductivity of PANI Materials

Sample	σ (Scm^{-1})
PANI	0.266
PANI–TiO_2	0.129
PANI–PVA	0.019
PANI–TiO_2–PVA	0.009

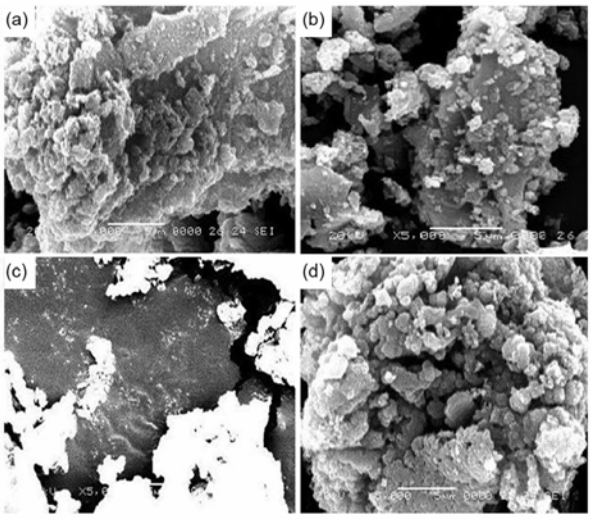

Fig.3—SEM images of (a) PANI, (b) PANI-TiO_2, (c) PANI-PVA and (d) PANI-TiO_2-PVA with ×10000 magnification

A summarization of physicochemical characteristics of all PANI composite materials inferred from the characterization studies just discussed is to be made here in order to understand the sensor behaviors of different PANI materials. Characteristics of pristine PANI are very much influenced by TiO_2 in the composite. Normal level of oxidation and hence the presence of almost equal number of quinoid and benzenoid groups, anatase crystalline structure, and lesser agglomerated grains are the characteristics of PANI-TiO_2 composite. These characteristics are altered by the addition of soft template PVA towards those of pristine PANI. Favorable aniline oxidation and outnumbering of quinoid groups, anatase structure with lesser *d*-space, and extensive agglomeration of particles/grains are the modified characteristics of PANI-TiO_2-PVA composite.

Figure 4 shows the sensor profiles of all the four polymer materials in static method for the vapors of solvents CH_3OH, CH_2Cl_2, CH_3CN and DMSO as a function of current. Table 3 compiles the sensor

Table 3—Sensor efficiencies in normalized conductivity change (η in %) of PANI materials on exposure to solvent vapors in static method

Sample	CH_3OH	CH_2Cl_2	CH_3CN	DMSO
PANI	56.0	-10.6	3.3	-3.3
PANI–TiO_2	7.9	-22.5	5.5	-3.4
PANI–PVA	-6.0	-24.7	6.7	-6.9
PANI–TiO_2–PVA	-61.0	-11.3	4.0	-8.3

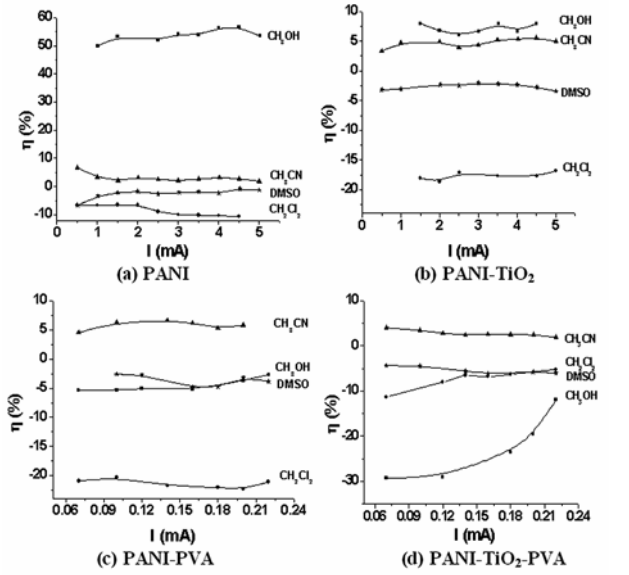

Fig. 4—Sensor profiles of polymer materials in static method at saturated vapor concentrations of different solvents, vaporization time = 30 min

efficiencies (in % of normalized voltage change- η). PANI shows the maximum sensor efficiency of 56% (with a decrease of its conductivity) for CH_3OH and for other solvents it has low η values. When TiO_2 or the soft template PVA is added separately, the sensor behavior of PANI is modified. CH_3OH sensing is reduced while CH_2Cl_2 sensing is improved but with a conductivity increase. As a result, both the PANI-TiO_2 and PANI-PVA materials show their maximum sensor efficiencies towards, CH_2Cl_2. Interestingly, however, when soft template PVA is added to PANI-TiO_2 composite, the resulting material PANI-TiO_2-PVA turns back its maximum sensor efficiency towards CH_3OH like PANI but with an increase of its conductivity (-61%). The sensor profiles obtained in dynamic method (Fig. 5) illustrate the static method trends very clearly. They also show conspicuously the reversibility in sensing process and regeneration of the sensor materials. All these observed results yield: (i) a particular PANI material behaves differently and characteristically in sensing of the vapors of various organic solvents, (ii) sensor behavior of pristine PANI gets modified in composite formation and (iii) sensor behavior when considered in relation with conductivity increase/decrease may involve different sensing mechanisms.

The trend in sensor behaviors of the four materials studied (Table 3) is in consistent with the different physicochemical characteristics. Notably, PANI-TiO_2 and PANI-TiO_2-PVA have different characteristics and different sensor behaviors. Similarly PANI and PANI-TiO_2-PVA materials although show their maximum sensor efficiencies toward CH_3OH, have different conductivity trends (decrease and increase in conductivity respectively) with CH_3OH vapor. Consequently they may have different underlying sensing mechanisms. Possibly pristine PANI accepts electron from CH_3OH through H-bonded electron donation (from O-H bond of methanol to amine/imine N of PANI) and hence through its conductivity decrease, it detects CH_3OH vapor. PANI-TiO_2-PVA, on the other hand, donates electron to CH_3OH (or other solvents') vapor (possibly through electrostatic bonding) and hence through its conductivity increase, the material senses CH_3OH vapor. The above plausible mechanisms also suggested in previous study[33] gets supportive evidence from the IR spectra of the materials in KBr pellet form, after their exposure to the solvent vapor. Figure 6 shows representatively such IR spectra for pristine PANI and PANI-TiO_2 composite, after exposure to CH_3OH and CH_2Cl_2 vapors respectively. There is a blue-shift in the quinoid peak of pristine PANI from 1602 cm^{-1} (before exposure, Fig. 1, spectrum a) to 1616 cm^{-1} after exposure. This blue-shift, i.e., shift to higher wave number indicates a greater bond energy, a greater bond strength and hence, an involvement of more number of electrons in bonding of quinoid group of PANI. This occurs when there is electron transfer from CH_3OH to imine moiety of quinoid group in PANI. Indirectly this causes a reduction in/loss of electron delocalization in PANI and hence

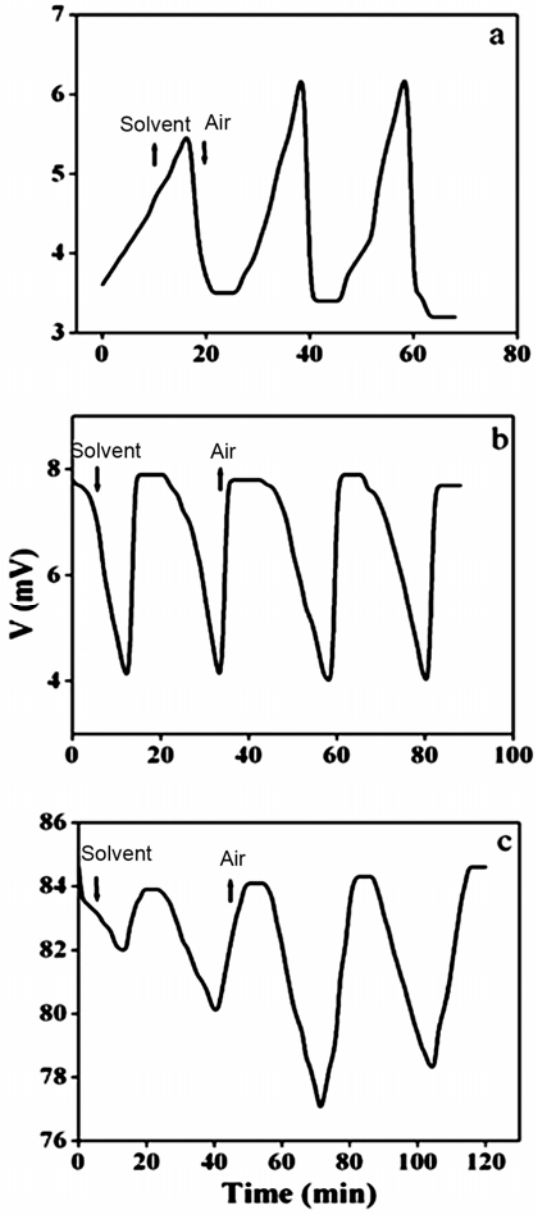

Fig. 5—Dynamic sensor behaviors of (a) PANI towards CH_3OH vapor–31 ppm, (b) PANI-TiO_2 towards CH_2Cl_2 vapor-11 ppm and (c) PANI-TiO_2-PVA towards CH_3OH vapor-55 ppm

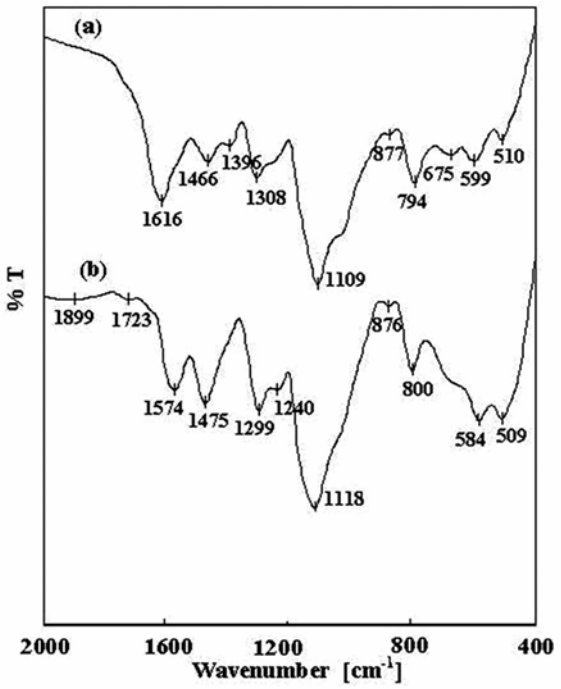

Fig. 6—FTIR spectra of (a) PANI after exposure to CH_3OH vapor and (b) PANI-TiO_2 after exposure to CH_2Cl_2 vapor

a conductivity decrease. Contrarily, a red-shift in quinoid and benzenoid peaks of PANI-TiO_2 composite is observed after its exposure to CH_2Cl_2 vapor. This red-shift indicates a lower bond energy, a weaker bond and hence an involvement of lesser number of electrons in bonding of quinoid and benzenoid groups of PANI-TiO_2 composite. This situation occurs when there is electron transfer from composite to solvent vapor, probably through electrostatic bonding (from negative surface charge centers of composite to partial positive charge centers of solvent molecule, e.g., $\delta+$ on H of CH_2Cl_2). Such act enhances electron delocalization in PANI chains and hence its conductivity.

The different sensing mechanisms of PANI in its pristine or composite forms and the underlying role played by TiO_2 or TiO_2-PVA combination in modifying/tuning pristine PANI characteristics could be understood as follows. PANI carries amine or protonated and positively charged imine groups while TiO_2 has surface hydroxyl group and negative charge[13], just complementary to PANI; similarly PVA also has –OH group. Hence, strong physicochemical interaction between PANI and TiO_2 through coulombic/hydrogen or coordination bonding[13,34] takes place and modifies PANI. Similar such inter-molecular hydrogen bonding from PVA also modifies PANI in PANI-PVA composite in similar lines with PANI-TiO_2 system. However, when PVA and TiO_2 are present together, their mutual interaction inhibits/influences their individual interaction with PANI, and thereby it imparts PANI-TiO_2-PVA material a characteristically different behavior.

Conclusions

In the present work organic-inorganic hybrid composites of conducting polyaniline with anatase TiO_2 have been successfully prepared by slightly modifying the conventional method with low-volume approach. Hybrid formation is confirmed by FTIR, XRD and SEM characterizations. Incorporation of TiO_2 modifies PANI to a chemically distinctive PANI-TiO_2 hybrid species so that its sensor behavior is tuned differently in comparison with PANI. Addition of soft template PVA, however, restores the sensor behavior of PANI in PANI-TiO_2-PVA but with an increase of its conductivity. Hence, PANI-TiO_2-PVA emerges as another hybrid material different from PANI-TiO_2. Thus TiO_2 or PANI-TiO_2 combination chemically modifies or tunes the characteristics of pristine PANI differently. The present work altogether points out clearly that materials with newer properties could be designed and fabricated from conducting polyaniline through composite formation with metallic oxide titania and/or PVA soft emplate.

Acknowledgements

Financial support provided by DST-SERC, Govt. of India through a project (No. SR/S2/CMP.22/2009) is gratefully acknowledged. One of the authors (NV) thanks UGC, New Delhi for the award of Teacher Fellowship under its XI plan Faculty Development Program.

References

1 Gangopadhyay R & De A, *Chem Mater*, 12 (2000) 608-622.
2 Rosoff M, *Nano-Surface Chemistry*, (Marcel Dekker, New York), 2002.
3 Xia H & Wang Q, *Chem Mater*, 14 (2002) 2158–2165.
4 Sanchez C, Julian B, Belleville P & Popall M, *J Mater Chem*, 15 (2005) 3559-3592.
5 Itoh T, Wang J, Matsubara I, Shin W, Izu N, Nishibori M & Murayama N, *Mater Lett*, 62 (2008) 3021-3023.
6 Lange U, Roznyatovskaya N V & Mirsky V M, *Anal Chim Acta*, 614 (2008) 1-26.
7 Zheng J, Li G, Ma X, Wang Y, Wu G & Cheng Y, *Sens Actuators B Chem*, 133 (2008) 374-380.
8 Karim M Z, Lee H W, Cheong I W, Park S M, Oh W & Yeum J H, *Polym Compos*, 31 (2010) 83-88.

9 Strohm H, Sgraja M, Bertling J & Lobmann P, *J Mater Sci*, 38 (2001) 1605-1609.

10 Gupta N, Sharma S, Mir I A & Kumar D, *J Sci Ind Res*, 65 (2006) 549-557.

11 Saini P, Choudhry V & Dhawan S K, *Indian J Eng Mater Sci*, 14 (2007) 436-442.

12 Chauhan N P S, Ameta R, Ameta R & Ameta S C, *Indian J Chem Technol*, 18 (2011) 118-122.

13 Das I, Gupta S K & Lall R S, 12 (2005) 198-204.

14 Sathiyanarayanan S, Syed Azim S & Venkatachari C, *Prog Org Coat*, 59 (2007) 291-296.

15 Liu Z, Zhou J, Xue H, Shen L, Zang H, Chen W, *Synth Met*, 156 (2006) 721-723.

16 Kim Y, Lim J W, Sung Y E, Xia J B, Masaki N & Yanagida S, *J Photochem Photobiol A Chem* , 204 (2009) 110-114.

17 Li X, Wang D, Cheng G, Luo Q, An J & Wang Y, *Appl Cat B Environ*, 81 (2008) 267-273.

18 Zhang H, Zong R, Zhao J & Zhu Y, *Environ Sci Technol*, 42 (2008) 3803-3807.

19 Phang S W, Tadokoro M, Watanabe J & Kuramoto N, *Curr Appl Phys*, 8 (2008) 391-394.

20 Yang Q, Tang K, Wang C, Qian Y, & Shuyuan Zhang S, *J Phys Chem B*, 106 (2002**)** 9227-9230.

21 Zhou Y, Shu H Y, Cui Y W, Xiao G L, Yu R Z, Zu Y C, *Adv Mater*, 11 (1999) 850-852.

22 Bhadra J, Sarkar D, *Mater Lett*, 63 (2009) 69-77.

23 Trivedi D C, in *Synthesis and Electrical properties*, *Handbook of Organic Conductive Molecules and Polymers*, edited by Nalwa H S, (John Wiely and Sons Ltd: Chichester), vol. 2, 1997, 505.

24 Murugesan R, Anitha G & Subramanian E, *Mater Chem Phys*, 85 (2004) 184-194.

25 Subramanian E, Anitha G, Karthik Selvam M & Ibrahim Ali, Badusha M, *Bull Mater Sci*, 28 (2005) 55-61.

26 Subramanian E, Anitha G & Vijayakumar N, *J Appl Polym Sci*, 106 (2007) 673-683.

27 Wieder H H, *Laboratory notes on electrical and galvanomagnetic measurements*, (Elseiver: Amsterdam), 1979, Ch 1, p 17.

28 Ping Z, Nauer G E, Neugebauer H, Theiner J & Neckel A, *J Chem Soc Faraday Trans*, 93 (1997) 121-129.

29 Boyer M I, Quillard S, Rebourt E, Louarn G, Buisson J P, Monkman A & Lefrant S J, *Phys Chem B*, 102 (1998) 7382-7392.

30 Qiu H, Qi S, Wang D, Wang J & Wu X, *Synth Met*, 160 (2010) 1179-1183.

31 Karim M R, Yeum J H, Lee M S & Lim K T, *Reactive Funct Polym*, 68 (2008) 1371-1376.

32 Bian C, Yu Y & Xue G, *J Appl Polym Sci*, 104 (2007) 21-26.

33 Lange U, Roznyatovskaya N V & Mirsky V M, *Anal Chim Acta*, 614 (2008) 1-26.

34 Li X W, Chen W, Bian C Q, He J B, Xu N & Xue G, *Appl Surf Sci*, 217 (2003) 16-22.